

- unit is defined as 1  $\mu\text{mol}$  of CO exchanged per min.
- CODH [120 to 140 mg ml<sup>-1</sup> in 50 mM tris-HCl (pH 7.6)] was reduced with CO (1 atm for 10 to 15 min) or with dithionite (4 mM final) and then methylated by adding the methylated corrinoid-FeS protein (1.5 to 2 equivalents) with vigorous shaking. The reaction mixture was placed in the RR sample holder and frozen cryogenically within 2 to 4 min after mixing the two proteins.
  - Treating the <sup>13</sup>CH<sub>3</sub> and <sup>12</sup>CH<sub>3</sub> groups as point masses of 16 and 15 amu, respectively, the calculated frequency ratio of the Ni-<sup>13</sup>CH<sub>3</sub> and Ni-<sup>12</sup>CH<sub>3</sub> stretching bands would be 0.975, which matches well with the observed value of 0.969. The calculated frequency ratio of the Ni-CD<sub>3</sub> and Ni-CH<sub>3</sub> stretching bands is 0.931, in agreement with the observed value of 0.927.
  - We also used CH<sub>3</sub>I as the methyl group donor to CODH. This reaction requires the intermediacy of the corrinoid-FeS protein, because the methylated corrinoid-FeS protein is the only known direct methyl donor for CODH (40). CODH [40 nmol, 6 mg, in 100  $\mu\text{l}$  of 50 mM tris-HCl (pH 7.6)] was mixed with 0.40 nmol of corrinoid-FeS protein under a CO atmosphere for 15 min. The atmosphere was exchanged with nitrogen, 4  $\mu\text{mol}$  of CH<sub>3</sub>I (20  $\mu\text{l}$  of 0.2 M) was added, and the solution was incubated for 30 min. Excess CH<sub>3</sub>I was removed by centrifuging the mixture through a Sephadex G-50 column, and the protein was concentrated with Amicon centricon tubes. By monitoring with tracer amounts of <sup>14</sup>CH<sub>3</sub>I, it was shown that 0.89 mol of methyl groups were incorporated per mol of CODH. When <sup>13</sup>CH<sub>3</sub>I was the methyl donor, the methyl-metal band was observed at 410 cm<sup>-1</sup>.
  - The calculated frequency ratio of the <sup>64</sup>Ni-<sup>12</sup>CH<sub>3</sub> and <sup>59</sup>Ni-<sup>12</sup>CH<sub>3</sub> stretching bands would be 0.990, which matches well with the observed value of 0.988. If an Fe-CH<sub>3</sub> bond had been observed, the position of the <sup>58</sup>Fe-CH<sub>3</sub> band would be expected to shift by 4 cm<sup>-1</sup> relative to the <sup>54</sup>Fe-CH<sub>3</sub> sample. Natural abundance Ni consists of <sup>58</sup>Ni and <sup>60</sup>Ni in ~2:1 ratio. The sharpness of the 417-cm<sup>-1</sup> band is interpreted to reflect the presence of a single Ni isotope. This provides further evidence that Ni is involved in this resonance.
  - S. W. Ragsdale, P. A. Lindahl, E. Münck, *J. Biol. Chem.* **262**, 14289 (1987); M. D. Wirt, M. Kumar, S. W. Ragsdale, M. R. Chance, *J. Am. Chem. Soc.* **115**, 2146 (1993). Unexpected generation of base-on Co<sup>2+</sup> (containing a coordinated benzimidazole base) would also be detectable because its spectrum is similar to that of base-off Co<sup>2+</sup> with the absorption envelope between 450 and 475 nm. In all the spectra, there is a contribution from the Fe-S clusters of CODH with a broad absorption between 350 and 420 nm. However, the spectra of the CODH clusters do not change significantly during the methylation reaction and the difference spectra are dominated by changes in the corrinoid spectra.
  - Stopped-flow experiments were performed on an Applied Photophysics spectrofluorimeter and data were fit with software purchased from Applied Photophysics. Solutions of enzymes and substrates were made in the anaerobic chamber, transferred into tonometers that are isolated from the atmosphere by stopcocks, and connected directly to the drive syringes of the stopped-flow instrument. These syringes were maintained anaerobically in a temperature-controlled bath of anaerobic water.
  - The possibility was ruled out that Co<sup>2+</sup> is the product of methyl transfer but is rapidly reduced to Co<sup>+</sup> by CODH in a subsequent step. In a separate experiment with the Co<sup>2+</sup>-corrinoid-FeS protein (5  $\mu\text{M}$ ) and CO-reduced CODH (2.5  $\mu\text{M}$ ), the  $k_{\text{obs}}$  for Co<sup>2+</sup> reduction was  $0.026 \pm 0.003 \text{ s}^{-1}$  at 30°C and  $0.037 \pm 0.003 \text{ s}^{-1}$  at 40°C. These rates are significantly lower than the rate of formation of Co<sup>+</sup> in the methyl transfer reaction. We and others earlier ruled out a mechanism involving one-electron reduction of methyl-Co<sup>3+</sup> followed by homolytic cleavage, which would also generate Co<sup>+</sup> [B. D. Martin and R. G. Finke, *J. Am. Chem. Soc.* **112**, 2419 (1990); S. A. Harder, W.-P. Lu, B. F. Feinberg, S. W. Ragsdale, *Biochemistry* **28**, 9080 (1989)].
  - We have found that the rate constant for methylation of CODH increases approximately twofold for every 10°C increase in temperature.
  - J. R. Roberts, W.-P. Lu, S. W. Ragsdale, *J. Bacteriol.* **174**, 4667 (1992).
  - M. D. Wirt *et al.*, *Biochemistry* **34**, 5269 (1995).
  - M. D. Wirt, I. Sagi, M. R. Chance, *Biophys. J.* **63**, 412 (1992); J. M. Pratt, in *Vitamin B<sub>12</sub>* D. Dolphin, Ed. (Wiley, New York, 1982), pp. 325–392.
  - G. C. Tucci and R. H. Holm, *J. Am. Chem. Soc.* **117**, 6489 (1995).
  - The order in which CO and the methyl group bind is not known. We favor a random mechanism because we have observed binary complexes of CODH with both CO and the methyl group. We also do not know which of the iron sites in the Fe-S component of center A binds CO.
  - B. D. Martin, S. A. Matchett, J. R. Norton, O. P. Anderson, *J. Am. Chem. Soc.* **107**, 7952 (1985).
  - R. P. Rosen *et al.*, *Organometallics* **3**, 846 (1984).
  - L. S. Hegedus, in *The Chemistry of the Metal-Carbon Bond. The Nature and Cleavage of Metal-Carbon Bonds*, F. R. Hartley and S. Patai, Eds. (Wiley, New York, 1985), vol. 2, pp. 401–512.
  - M. S. Ram and C. G. Riordan, *J. Am. Chem. Soc.* **117**, 2365 (1995).
  - J. J. Alexander, in (32), pp. 339–400.
  - D. J. Forster, *J. Am. Chem. Soc.* **98**, 846 (1976); *Adv. Organomet. Chem.* **17**, 255 (1979).
  - F. W. Sunderman, Ed., *Nickel in the Human Environment* (Oxford Univ. Press, New York, 1985).
  - B. M. Babior, *BioFactors* **1**, 21 (1988); R. G. Finke, in *Molecular Mechanisms in Bioorganic Processes* (Royal Society of Chemistry, London, 1990), pp. 244–279; R. G. Matthews, R. V. Banerjee, S. W. Ragsdale, *BioFactors* **2**, 147 (1990).
  - A. Berkessel, *Bioorg. Chem.* **19**, 101 (1991); H. C. Friedmann, A. Klein, R. K. Thauer, *FEMS Microbiol. Rev.* **87**, 339 (1990).
  - S. W. Ragsdale, P. A. Lindahl, E. Münck, *J. Biol. Chem.* **262**, 14289 (1987).
  - W.-P. Lu, S. R. Harder, S. W. Ragsdale, *ibid.* **265**, 3124 (1990).
  - Supported by grant GM39451 (S.W.R.) and grant GM 13498 (T.G.S.) from the National Institutes of Health.

9 June 1995; accepted 8 August 1995

## T Cell Awareness of Paternal Alloantigens During Pregnancy

Anna Tafuri, Judith Alferink, Peter Möller, Günter J. Hämmerling, Bernd Arnold\*

During pregnancy a semiallogeneic fetus survives despite the presence of maternal T cells specific for paternally inherited histocompatibility antigens. A mouse transgenic for a T cell receptor recognizing the major histocompatibility (MHC) antigen H-2K<sup>b</sup> was used to follow the fate of T cells reactive to paternal alloantigens. In contrast to syngeneic and third-party allogeneic pregnancies, mice bearing a K<sup>b</sup>-positive conceptus had reduced numbers of K<sup>b</sup>-reactive T cells and accepted K<sup>b</sup>-positive tumor grafts. T cell phenotype and responsiveness were restored after delivery. Thus, during pregnancy maternal T cells acquire a transient state of tolerance specific for paternal alloantigens.

In outbred species, inheritance of paternal histocompatibility antigens by the embryo results in genetic mismatches to the mother. The semiallogeneic fetus is in direct physical contact with uterine and blood-borne cells of the mother, and fetal rejection by the maternal immune system is prevented by mechanisms as yet undefined (1). In mice, midgestational placenta expresses paternal MHC antigens of the K and D loci (1, 2); when grafted into maternal-strain recipients, it is rejected and induces sensitization to paternal alloantigens (3). However, neither ignorance nor tolerance of maternal T cells to paternal alloantigens has been conclusively shown. Impairment of T cell responses has been observed, but its selectivity to paternal alloantigens remains controversial (1, 4, 5). Midpregnant CBA mice, which are inbred, have unaltered expression of T cell receptor (TCR), CD4, and CD8 (6). However, phe-

notypic changes may go undetected because T cells specific for paternal alloantigens have low frequency in a normal T cell repertoire. Here, we used a TCR transgenic mouse model (Des-TCR) harboring a T cell repertoire skewed toward the paternal alloantigen H-2K<sup>b</sup> (7) to take advantage of the high frequency of allospecific cytotoxic T cells as well as the ease of monitoring the transgenic TCR with clonotype-specific antibodies.

Virgin H-2<sup>k</sup> Des-TCR transgenic females were mated with H-2<sup>b</sup> C57BL/6 males, and K<sup>b</sup>-specific T cells were phenotypically characterized during pregnancy. Nonspecific gestational effects (8) were controlled for by syngeneic and third-party allogeneic matings with H-2<sup>k</sup> CBA or H-2<sup>s</sup> ASW males (9), respectively. Midpregnant Des-TCR mice bearing a K<sup>b</sup>-positive conceptus had reduced numbers of T cells with high expression of the clonotype (Fig. 1B, left) and six to nine times more clonotype-positive cells devoid of CD4 and CD8 (Fig. 1B, right) when compared to the results obtained for H-2<sup>k</sup> syngeneic (Fig. 1C) and H-2<sup>s</sup> third-party allogeneic (Fig. 1D) pregnancies. Therefore, maternal T cells specifically recognize paternal alloantigens.

A. Tafuri, J. Alferink, G. J. Hämmerling, B. Arnold, Tumor Immunology Program, Deutsches Krebsforschungszentrum (DKFZ), Im Neuenheimer Feld 280, 69120 Heidelberg, Germany.  
P. Möller, Institute of Pathology, University of Heidelberg, Im Neuenheimer Feld 220, 69120 Heidelberg, Germany.

\*To whom correspondence should be addressed.

To determine whether T cell phenotypic changes in response to paternal  $K^b$  persist after delivery, we mated thymectomized  $H-2^k$  Des-TCR females with  $H-2^b$  C57BL/6 males. During midpregnancy, clonotype-positive T cells underwent phenotypic alterations (Fig. 2B) similar to those of non-thymectomized mice (Fig. 1B). After delivery, the expression of the clonotype, CD4, and CD8 in  $K^b$ -specific T cells (Fig. 2C) did not differ from that of control mice (Fig.

2A). Therefore, the alterations of mature peripheral T cells occur extrathymically and are reversed after delivery in the absence of a new thymic T cell input (10).

To dissect the role of B cells and  $CD4^+$  T cells during pregnancy, we used Des-TCR SCID (severe combined immunodeficiency disease) mice. SCID mice are unable to autonomously rearrange immunoglobulin (Ig) and TCR genes but normally express a rearranged transgenic TCR (11). The pe-

ripheral lymphoid organs of  $H-2^{d \times k}$  Des-TCR SCID mice were devoid of B cells, T cells expressing TCRs other than the transgenic clonotype, and  $CD4^+Des^+$  T cells (Fig. 3B); this observation supports the hypothesis that the expression of a second TCR is required for positive selection of  $CD4^+Des^+$  T cells (12). When mated with C57BL/6 males,  $H-2^{d \times k}$  Des-TCR SCID mice gave birth to healthy litters of comparable size to those from syngeneic matings. Clonotype expression was reduced in  $H-2^b$  allogeneic pregnancies (Fig. 3D) in comparison with syngeneic pregnancies (Fig. 3E). Therefore, the encounter with paternal  $K^b$  is per se sufficient to perturb the phenotype of  $CD8^+Des^+$  T cells, which rules out the hypotheses that fetal rejection is prevented by alloantibodies masking paternal MHC class I antigens on fetal target cells (13) and that  $CD4^+$  T cells are of critical importance for successful pregnancies in this model. Production of cytokines such as transforming growth factor- $\beta 2$  (14), interleukin (IL)-4, and IL-10 at the fetomaternal interface may induce  $T_H2$ -type  $CD4^+$  T cells, thereby improving fetal survival (15). In Des-TCR SCID mice,  $CD8^+$  T cells may have a similar function, as  $CD8^+$  T cells reportedly produce heterogeneous patterns of cytokines (16). To assess whether placental sequestration accounted for the reduction of T cells expressing high clonotype levels, we analyzed fetoplacental tissues from midpregnant Des-TCR SCID mice by immunohistology.  $CD8^+Des^+$  T cells were absent from placental and embryonic tissues during  $H-2^b$  allogeneic and syngeneic pregnancies (17); thus, clonotype-positive T cells were not trapped in the placenta. The site where T cells encounter paternal  $K^b$  remains undefined. Fetal cells leaking into the maternal circulation may provide an alternative source of paternal alloantigens (18).

To investigate whether tolerance to paternal alloantigens is induced during pregnancy and then reversed after delivery because of antigen elimination (19), we overlapped the putative window of tolerance with the immune challenge and used a phenomenon no longer reversible after the decline of tolerance as a readout system. The growth of P815- $K^b$  tumor grafts was the criterion for  $K^b$ -specific T cell tolerance, because  $K^b$ -transfected  $H-2^d$  P815 mastocytoma cells are rejected by  $K^b$ -specific T cells in  $H-2^{d \times k}$  Des-TCR mice and are accepted by  $K^b$ -tolerant mice (20). P815- $K^b$  cells administered at the time of fetal implantation (8) generated a  $K^b$ -positive tumor mass in Des-TCR mice bearing a  $K^b$ -positive conceptus, but they were usually rejected during syngeneic and third-party allogeneic pregnancies (Fig. 4). P815- $K^b$  tumor growth was also

**Fig. 1.** Midgestational changes of  $K^b$ -specific T cell phenotype in response to paternal  $K^b$ . Three-color cytofluorimetric analyses (9) of B cell-depleted splenocytes from nonpregnant mice (A) and from midpregnant (days 9 to 11)  $H-2^k$  Des-TCR mice during  $H-2^b$  allogeneic pregnancies (B),  $H-2^k$  syngeneic pregnancies (C), and third-party  $H-2^s$  allogeneic pregnancies (D) are shown. Histograms represent clonotype expression; dot plots represent CD4 versus CD8 expression on gated clonotype-positive T cells. The data are representative of four experiments.

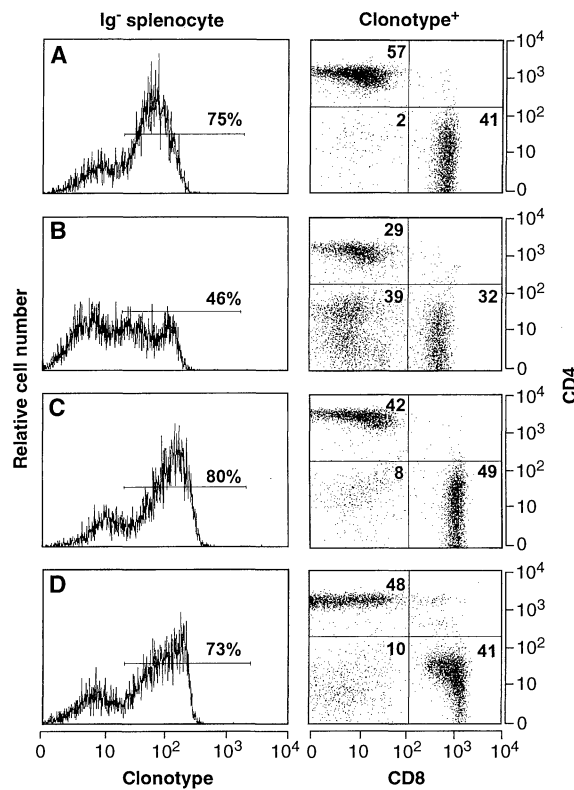
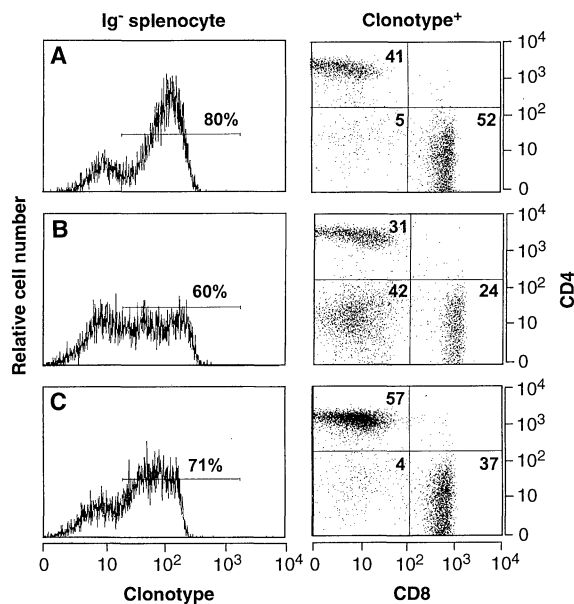


**Fig. 2.** Extrathymic occurrence and postpartum reversibility of T cell phenotypic changes in response to paternal  $K^b$ . Three-color cytofluorimetric analyses of B cell-depleted splenocytes (9) from adult thymectomized  $H-2^k$  Des-TCR mice under control conditions (A), on day 10 of  $H-2^b$  allogeneic pregnancies (B), and 3 days after delivery (C) are shown. Histograms represent clonotype expression; dot plots represent CD4 versus CD8 expression on gated clonotype-positive T cells. Thymectomy was performed at 4 weeks of age. The data are representative of three experiments.



observed in four of five Des-TCR mice injected on days 10 to 11 of H-2<sup>b</sup> allogeneic pregnancies. After delivery (21 to 28 days), the ability to reject P815-K<sup>b</sup> grafts was restored (four of four allogeneic pregnancies and three of three syngeneic pregnancies). Because K<sup>b</sup>-positive tumor grafts were only accepted in the presence of a K<sup>b</sup>-positive fetus, we conclude that pregnancy induces a transient state of T cell tolerance specific for the paternal alloantigens.

During pregnancy, paternal grafts may survive only if they bear MHC-peptide complexes identical to those of the fetus. Mismatches resulting from graft expression of tissue-specific peptides may recruit T cells reactive to these "nonfetal" components and may lead to graft rejection. Un-

like mice harboring a normal T cell repertoire, Des-TCR transgenic mice may be unable to mount such responses because their repertoire is skewed toward the "tolerant" allospecificity (21). Recognition of maternal MHC-peptide complexes expressed by the fetus may theoretically block harmful T cell reactions against maternal autoantigens (22). Such extended T cell "awareness" to fetal components could in part explain why certain autoimmune diseases, such as multiple sclerosis and rheumatoid arthritis, undergo remission during pregnancy (23), apparently in the absence of general immunosuppression. If this hypothesis were true, understanding the unique features of T cell interactions with fetal cells would provide a

powerful tool to reinstruct the immune system in the course of autoimmune diseases and transplant rejection.

## REFERENCES AND NOTES

1. T. J. I. Gill, *Crit. Rev. Immunol.* **5**, 201 (1984); D. A. Clark, *ibid.* **11**, 215 (1991); G. Chaouat, in *Immunology of Pregnancy*, G. Chaouat, Ed. (CRC Press, Boca Raton, FL, 1993), pp. 1-17.
2. M. L. Hedley, B. L. Drake, J. R. Head, P. W. Tucker, J. Forman, *J. Immunol.* **142**, 4046 (1989); R. Raghupathy, B. Singh, J. Barrington-Leigh, T. G. Wegmann, *ibid.* **127**, 2074 (1981).
3. R. L. Simmons and P. S. Russell, *Ann. N.Y. Acad. Sci.* **99**, 717 (1962).
4. M. O'Hearn and H. R. Hilgard, *Transplantation* **32**, 389 (1981); S. Nicklin and W. D. Billington, *Clin. Exp. Immunol.* **49**, 135 (1982); C. S. Pavia and D. P. Stites, *J. Immunol.* **123**, 2194 (1979); M. Parvin, K. Isobe, S. Goto, I. Nakashima, Y. Tomoda, *Microbiol. Immunol.* **36**, 757 (1992); G. A. Voisin, *Folia Biol. (Prague)* **40**, 505 (1994).
5. N. Fabris, L. Piantanelli, M. Muzzioli, *Clin. Exp. Immunol.* **28**, 306 (1977).
6. All animals were kept under specific pathogen-free conditions. Allogeneic and syngeneic pregnancies were obtained by mating virgin H-2<sup>k</sup> CBA females with H-2<sup>b</sup> C57BL/6 and CBA males, respectively. A doubling of the number of total (5) and B cell-depleted splenocytes was observed during both allogeneic and syngeneic midpregnancies. Three-color cyto-fluorimetric analysis (9) revealed unchanged expression of TCR $\alpha\beta$ , CD4, and CD8.
7. G. Schönrich *et al.*, *Cell* **65**, 293 (1991).
8. J. C. Cross, Z. Werb, S. J. Fisher, *Science* **266**, 1508 (1994).
9. Mating of Des-TCR mice with C57BL/6 males resulted in healthy litters of normal size. H-2<sup>s</sup> ASW mice were selected as third-party allogeneic partners because T cells from Des-TCR mice do not respond to ASW stimulators in mixed leukocyte reactions. An increase in the number of total ( $60 \times 10^6$  versus  $120 \times 10^6$  mean value) and B cell-depleted ( $35 \times 10^6$  versus  $59 \times 10^6$  mean value) splenocytes was observed in midpregnant Des-TCR mice, irrespective of the male partner. Splenocyte counts reverted to normal after delivery. Splenocytes depleted of IgG-coupled to magnetic beads (sheep antibody to mouse IgG coupled to magnetic beads) were stained with the clonotype-specific Désiré-1 (7) monoclonal antibody (mAb) and with commercial (Gibco) mAbs specific for CD4 (H129.19), CD8 (53-6.7), and TCR $\alpha\beta$  (H57-597). Biotinylated mAbs were revealed by streptavidin-Red 670 (Gibco). Analysis was performed on a FACScan cytometer (Becton Dickinson).
10. Pregnancy does not result in the permanent elimination of T cells specific for paternal alloantigens. However, the mechanisms responsible for the phenotypic alterations of K<sup>b</sup>-specific T cells remain buried in the nonspecific fluctuations of spleen cell numbers typical of pregnancy (9). Reduction of Des-TCR T cells during midpregnancy may theoretically result from peripheral deletion, TCR down-regulation, or both. Restoration of the T cell phenotype after delivery may derive from up-regulation of TCR, CD4/CD8, or both, or from peripheral expansion of T cells maintaining high clonotype expression.
11. B. Scott, H. Blüthmann, H. S. Teh, H. von Boehmer, *Nature* **338**, 591 (1989).
12. E. Padovan *et al.*, *Science* **262**, 422 (1993); W. R. Heath and J. F. A. P. Miller, *J. Exp. Med.* **178**, 1807 (1993).
13. C. M. Hetherington and D. W. Dresser, *Immunology* **71**, 449 (1990); N. E. Herrera-Gonzalez and D. W. Dresser, *Dev. Comp. Immunol.* **17**, 1 (1993).
14. D. A. Clark *et al.*, *J. Immunol.* **144**, 3008 (1990).
15. S. Delassus, G. C. Coutinho, C. Saucier, S. Darce, P. Kourilsky, *ibid.* **152**, 2411 (1994); T. G. Wegmann, H. Lin, L. Guilbert, T. R. Mosmann, *Immunol. Today* **14**, 353 (1993).
16. S. Sad, R. Marcotte, T. R. Mosmann, *Immunity* **2**, 271 (1995).
17. Immunohistochemistry was performed on shock-frozen sections of uteri from H-2<sup>d<sup>k</sup></sup> Des-TCR SCID

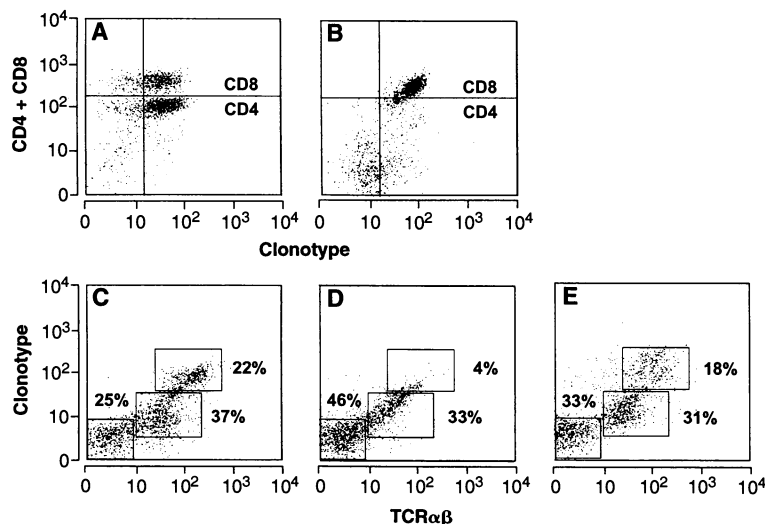
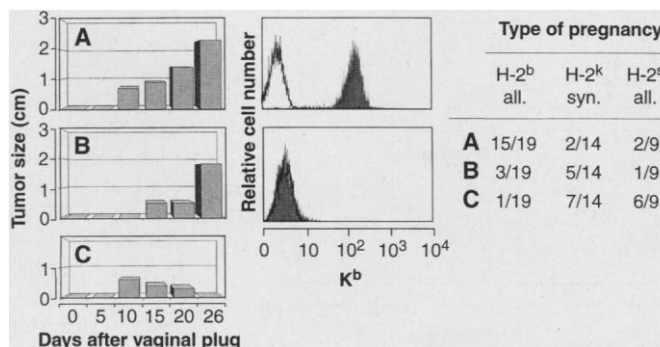


**Fig. 3.** Phenotypic alterations of CD8<sup>+</sup>Des<sup>+</sup> T cells in response to paternal K<sup>b</sup> in Des-TCR SCID mice. **(A and B)** Peripheral lymphoid organs of Des-TCR SCID mice are devoid of CD4<sup>+</sup>Des<sup>+</sup> T cells. Dot plots represent clonotype versus CD4 and CD8 expression on B cell-depleted lymph nodes from H-2<sup>d<sup>k</sup></sup> Des-TCR mice **(A)** and total lymph node cells from H-2<sup>d<sup>k</sup></sup> Des-TCR SCID mice **(B)**. **(C through E)** Dot plots represent TCR $\alpha\beta$  versus clonotype expression on splenocytes from nonpregnant mice **(C)** and from midpregnant H-2<sup>d<sup>k</sup></sup> Des-TCR SCID mice bearing H-2<sup>b</sup> allogeneic **(D)** or syngeneic **(E)** concepti. The data are representative of three experiments.

**Fig. 4.** Impaired rejection of K<sup>b</sup>-positive tumor grafts by Des-TCR mice bearing a K<sup>b</sup>-positive conceptus. H-2<sup>d<sup>k</sup></sup> Des-TCR mice were challenged with  $1 \times 10^5$  P815-K<sup>b</sup> tumor cells on days 3 to 5 of H-2<sup>b</sup> allogeneic, H-2<sup>k</sup> syngeneic, or third-party H-2<sup>s</sup> allogeneic pregnancies. Representative examples of growth kinetics (left) and K<sup>b</sup> expression of P815-K<sup>b</sup> cells *ex vivo* (right) are shown. Three types of effects were observed: growth of a K<sup>b</sup>-positive tumor **(A)**, growth of a K<sup>b</sup>-negative loss variant **(B)**, and rejection **(C)**; the table shows the incidence of these effects for the three pregnancy types.



Because  $\geq 95\%$  of injected P815-K<sup>b</sup> cells expressed K<sup>b</sup>, the growth of the K<sup>b</sup>-negative variants resulted from rejection of K<sup>b</sup>-positive cells and *in vivo* immune selection. K<sup>b</sup>-specific T cell responsiveness was significantly impaired ( $P \leq 0.05$ , Fisher exact test) during H-2<sup>b</sup> allogeneic pregnancies when compared to syngeneic ( $P = 0.004$ ) and third-party allogeneic ( $P = 0.04$ ) pregnancies.

- mice carrying H-2<sup>b</sup> allogeneic or H-2<sup>k</sup> syngeneic pregnancies (day 10). Leukocytes were identified by a CD45-specific mAb (30F11.1, Pharmingen); T cells were identified by an unconjugated rat clonotype-specific mAb (B20.2.2) and by commercial (Gibco) biotinylated mAbs specific for CD3 (29B) and TCR $\alpha\beta$  (H57-597). Unconjugated primary antibodies were detected with a biotinylated sheep antibody to rat serum. Biotinylated antibodies were revealed by a streptavidin-biotinylated peroxidase complex. The numbers of CD45-positive cells were comparable in midpregnant allogeneic and syngeneic uteri. Maternal T cells were numerous in the decidua but were absent from the placenta and fetus.
18. P. J. M. Philip, N. Ayraud, R. Masseyef, *Immunol. Lett.* **4**, 175 (1982). K<sup>b</sup>-positive cells (0.01 to 0.27%) were detected in the blood but not in lymphoid organs of H-2<sup>k</sup> Des-TCR mice during H-2<sup>b</sup> allogeneic midpregnancies. Biotinylated K10-56.1, revealed by streptavidin-phycoerythrin, and propidium iodide were used for staining.
  19. F. Ramsdell and B. J. Fowlkes, *Science* **257**, 1130 (1992); J. Alferink, B. Schitteck, G. Schönrich, G. J. Hämmerling, B. Arnold, *Int. Immunol.* **7**, 331 (1995).
  20. H-2<sup>d</sup> P815-K<sup>b</sup> mastocytoma cells implanted subcutaneously are rejected by H-2<sup>d</sup> $\times$ k Des-TCR mice but are accepted by Des-TCR mice tolerant to K<sup>b</sup> expressed under the Keratin-IV promoter (2.4Ker.K<sup>b</sup>  $\times$  Des-TCR) (24). P815-K<sup>b</sup> elimination is mediated by Des-TCR T cells. *In vivo* depletion of Des-TCR T cells by Désiré-1 mAb, but not of natural killer cells by NK1.1 mAb, blocked tumor rejection (A. Limmer, G. J. Hämmerling, B. Arnold, unpublished data). Rejection was verified for more than 3 months. When the tumor diameter exceeded 2 cm after increasing for more than two consecutive measurements, tumor-bearing mice were killed, and K<sup>b</sup> expression was tested on P815-K<sup>b</sup> cells *ex vivo*.
  21. Among all peptides extracted from K<sup>b</sup> molecules [C57BL/6 spleen, EL-4, or RMA (H-2<sup>b</sup>) tumor cells] and separated by high-performance liquid chromatography, only one and the same peptide fraction sensitized RMA-S cells for recognition by a Des-TCR-positive clone. Therefore, the Des-TCR-positive clone recognizes only one (or few) peptides in the context of K<sup>b</sup>. The peptide sequence is currently being investigated (A. Guimezanés and A.-M. Schmitt-Verhulst, personal communication).
  22. T. M. Pribyl *et al.*, *Proc. Natl. Acad. Sci. U.S.A.* **90**, 10695 (1993).
  23. G. T. Waites and A. Whyte, *Clin. Exp. Immunol.* **67**, 467 (1987); O. Abramsky, I. Lubetzky-Korn, S. Evron, T. Brenner, *Prog. Clin. Biol. Res.* **12**, 695 (1984); M. W. Varner, *Semin. Perinatol.* **15**, 238 (1991).
  24. G. Schönrich *et al.*, *Int. Immunol.* **4**, 581 (1992).
  25. We thank J. Weik, A. Klevenz, G. Küblbeck, S. Schmitt, and S. Westenfelder for technical assistance, T. Meinhardt for help with the figures, B. Malissen for mAb B20.2.2, and L. Edler for statistical analysis. Supported by grants from Deutsche Forschungsgemeinschaft (Ar 152/3-1) and HCM Network (ERBCHRXCT 920008).

15 May 1995; accepted 8 August 1995

## Relaxation of Arterial Smooth Muscle by Calcium Sparks

M. T. Nelson, H. Cheng, M. Rubart, L. F. Santana, A. D. Bonev, H. J. Knot, W. J. Lederer\*

Local increases in intracellular calcium ion concentration ( $[Ca^{2+}]_i$ ) resulting from activation of the ryanodine-sensitive calcium-release channel in the sarcoplasmic reticulum (SR) of smooth muscle cause arterial dilation. Ryanodine-sensitive, spontaneous local increases in  $[Ca^{2+}]_i$  ( $Ca^{2+}$  sparks) from the SR were observed just under the surface membrane of single smooth muscle cells from myogenic cerebral arteries. Ryanodine and thapsigargin inhibited  $Ca^{2+}$  sparks and  $Ca^{2+}$ -dependent potassium ( $K_{Ca}$ ) currents, suggesting that  $Ca^{2+}$  sparks activate  $K_{Ca}$  channels. Furthermore,  $K_{Ca}$  channels activated by  $Ca^{2+}$  sparks appeared to hyperpolarize and dilate pressurized myogenic arteries because ryanodine and thapsigargin depolarized and constricted these arteries to an extent similar to that produced by blockers of  $K_{Ca}$  channels.  $Ca^{2+}$  sparks indirectly cause vasodilation through activation of  $K_{Ca}$  channels, but have little direct effect on spatially averaged  $[Ca^{2+}]_i$ , which regulates contraction.

Myogenic arteries control blood flow in the brain and respond to changes in intravascular pressure. Increased intravascular pressure causes a graded membrane potential depolarization of smooth muscle cells and arterial constriction (myogenic tone)

M. T. Nelson, A. D. Bonev, H. J. Knot, Department of Pharmacology, 55A South Park Drive, University of Vermont, Colchester, Vermont 05446, USA.

H. Cheng, L. F. Santana, W. J. Lederer, Department of Physiology and The Medical Biotechnology Center, University of Maryland School of Medicine, 660 West Redwood Street, Baltimore, MD 21201, USA.

M. Rubart, Krannert Institute of Cardiology, Indiana University School of Medicine, Indianapolis, IN 46202-4800, USA.

\*To whom correspondence should be addressed.

(1-3). Small, pressurized cerebral arteries dilate when the membrane potential of the smooth muscle cells is made more negative over the physiological range of membrane potentials (-60 to -30 mV), because steady  $Ca^{2+}$ -influx through dihydropyridine-sensitive, voltage-dependent  $Ca^{2+}$  channels declines (2-4).  $Ca^{2+}$  entry at physiological membrane potentials affects spatially averaged  $[Ca^{2+}]_i$  in arterial smooth muscle (3, 4). Although ryanodine-sensitive  $Ca^{2+}$ -release channels directly contribute to the global  $[Ca^{2+}]_i$  transient and contraction in cardiac muscle (5), their functional role in smooth muscle has not been established (4, 6, 7). We monitored ele-

mentary ryanodine-sensitive  $Ca^{2+}$ -release events ( $Ca^{2+}$  sparks) from smooth muscle SR by measuring rapid local changes in  $[Ca^{2+}]_i$  in smooth muscle cells isolated from resistance-sized cerebral arteries. We provide evidence that ryanodine-sensitive  $Ca^{2+}$ -release channels in smooth muscle SR, unlike their counterparts in cardiac and skeletal muscle, have a central role in limiting muscle contraction by activating  $K_{Ca}$  channels.

Single smooth muscle cells were isolated enzymatically from myogenic cerebral (100- to 150- $\mu$ m in diameter posterior and middle cerebral) arteries from rat (8). We used a laser scanning confocal microscope and the fluorescent  $Ca^{2+}$  indicator fluo-3 (9) to detect  $Ca^{2+}$  sparks in single cells bathed in physiological salt solution (Figs. 1 and 2). The mean rise-time and half-time of decay of  $Ca^{2+}$  sparks were  $20.2 \pm 2.3$  ms and  $48.0 \pm 2.6$  ms ( $n = 11$ ), respectively (Fig. 1). The mean peak  $[Ca^{2+}]_i$  during the  $Ca^{2+}$  spark was  $303 \pm 27$  nM (assuming 100 nM resting  $Ca^{2+}$ ) (Fig. 1) (10). The mean spread of the spark at the peak was  $2.38 \pm 0.14$   $\mu$ m ( $n = 11$ ) (Fig. 1) (10), corresponding to 0.8% of the surface area of the cell membrane (11).

Ryanodine, which inhibits SR  $Ca^{2+}$ -release channels at micromolar concentrations (5, 6), blocked  $Ca^{2+}$  sparks in smooth muscle cells (Fig. 2B).  $Ca^{2+}$  sparks were not observed in cells exposed to 10  $\mu$ M ryanodine and the  $Ca^{2+}$  channel agonist Bay K 8644, whereas 88% of cells treated with Bay K 8644 alone had  $Ca^{2+}$  sparks.  $Ca^{2+}$  sparks were not observed in cells exposed to thapsigargin (1  $\mu$ M), which inhibits  $Ca^{2+}$  uptake into the SR by the  $Ca^{2+}$ -ATPase (12). Application of cadmium (200  $\mu$ M), which immediately blocks voltage-dependent  $Ca^{2+}$  channels, did not immediately block  $Ca^{2+}$  sparks in our cells ( $n = 7$ ), a finding similar to that observed in quiescent heart muscle cells (5). However, prolonged exposure to Bay K 8644 increased  $Ca^{2+}$ -spark occurrence (Fig. 2B). The majority of  $Ca^{2+}$  sparks (59%) arose close to the sarcolemmal surfaces (within 1  $\mu$ m) of the smooth muscle cells (Fig. 2C). The  $Ca^{2+}$  sparks that were detected in the middle of the line-scan may still have arisen at the sarcolemmal surface because smooth muscle cells have infoldings of the surface membranes (caveolae). These results suggest that most  $Ca^{2+}$  sparks in smooth muscle cells from resistance-sized cerebral arteries result from the opening of ryanodine-sensitive  $Ca^{2+}$ -release channels in SR just under the cell membrane.

The proximity of the  $Ca^{2+}$  sparks to the cell surface raises the possibility that the  $Ca^{2+}$  spark serves as an intracellular signal to the sarcolemmal membrane.  $Ca^{2+}$ -activated  $K^+$  ( $K_{Ca}$ ) channels that exist in this membrane (2, 3) should be activated by the